BP-1-102 exerts antitumor effects on T-cell acute lymphoblastic leukemia cells by suppressing the JAK2/STAT3/c-Myc signaling pathway

CAN YE[1-3], XUEQIN RUAN[1-3], YAN ZHAO[1-3], HONGKAI ZHU[1-3], CANFEI WANG[1-3], ZHAO CHENG[1-3] and HONGLING PENG[1-4]

[1]Department of Hematology, The Second Xiangya Hospital; [2]Institute of Molecular Hematology, Central South University; [3]Hunan Engineering Research Center of Targeted Therapy for Hematopoietic Malignancies; [4]Hunan Key Laboratory of Tumor Models and Individualized Medicine, The Second Xiangya Hospital, Central South University, Changsha, Hunan 410000, P.R. China

Received September 30, 2022; Accepted February 17, 2023

DOI: 10.3892/etm.2023.11890

Abstract. Drug resistance and relapse of T-cell acute lymphoblastic leukemia (T-ALL) remain significant concerns for physicians; hence, the development and screening of effective targeted drugs remain important. Considering that STAT3 is emerging as a potential therapeutic target for T-ALL, T-ALL cell lines (MOLT-4 and CUTLL1) were treated with BP-1-102, a small-molecule inhibitor that blocks STAT3 phosphorylation. Cell Counting Kit-8 assay and colony formation assay results showed that BP-1-102 inhibited T-ALL cell proliferation and colony formation. Flow cytometry and morphological results demonstrated that BP-1-102 dramatically induced apoptosis and caused cell cycle arrest at the G_0/G_1 phase in T-ALL cell lines. Western blotting results indicated that BP-1-102 suppressed the JAK2/STAT3/c-Myc pathway activity in T-ALL cell lines. In conclusion, BP-1-102 suppressed the JAK2/STAT3/c-Myc signaling pathway in T-ALL cells and exerted various antitumor effects, representing a promising targeted antitumor inhibitor.

Introduction

T-cell acute lymphoblastic leukemia (T-ALL) is a hematological malignancy with marked heterogeneity. A variety of genetic mutations or chromosomal variations lead to the malignant transformation of T-cell progenitors and define different subtypes (1,2). In Europe, the USA and Japan, T-ALL accounts for 10-15% of pediatric ALL cases and 20-25% of adult ALL cases. Since the introduction of intensive chemotherapy, the remission rate for T-ALL is increasing, and the prognosis is gradually improving. Unfortunately, T-ALL relapse remains a significant concern (1,3,4). Highly aggressive relapsed T-ALL has a poor prognosis and is generally resistant to chemotherapy (5-7). In the face of these clinical challenges, researchers are committed to identifying more specific therapeutic targets and developing more effective and less toxic anti-leukemia drugs or drug combinations.

The Janus kinase/signal transducer and activator of transcription (JAK/STAT) signaling pathway is a signaling hub that mediates the intracellular signaling of a variety of cytokines and growth factors. Its aberrant activation is associated with a variety of hematological malignancies (8-10). Inhibition of the JAK/STAT pathway holds promise for the treatment of a range of diseases, and several inhibitors of the JAK/STAT pathway are currently being tested in clinical trials (8). Most STAT3 small-molecule inhibitors block STAT3 phosphorylation and/or dimerization. Several STAT3 inhibitors, including STX-0119, STA-21, LLL-3, LLL12, XZH-5, and OPB-31121, exhibit antitumor properties, but few have been approved for clinical trials or clinical use (11-16).

BP-1-102, an orally available inhibitor of STAT3 phosphorylation, blocks STAT3 phosphorylation and dimerization by directly interfering with the binding of phosphorylated tyrosine residue (pTyr) of the upstream molecule to the Src homology 2 (SH2) domain of STAT3. BP-1-102 reduces phosphorylated STAT3 levels in cells and subsequently inhibits the expression of its downstream proteins c-Myc, Bcl-xL, Cyclin D1, Survivin and VEGF, thereby suppressing the growth, survival, migration and invasion of tumor cells (17). BP-1-102 exerts antitumor effects in several solid tumor cell lines, including breast cancer, non-small cell lung cancer and gastric adenocarcinoma (17-19).

Although the majority of ALL is B-ALL, there is a greater need for targeted therapies for T-ALL. Our preliminary results

Correspondence to: Dr Zhao Cheng or Professor Hongling Peng, Department of Hematology, The Second Xiangya Hospital, Central South University, 139 Renmin Road, Furong, Changsha, Hunan 410000, P.R. China
E-mail: chengzhao@csu.edu.cn
E-mail: penghongling@csu.edu.cn

Key words: T-cell acute lymphoblastic leukemia, STAT3, small-molecule inhibitor, proliferation, colony formation, apoptosis, cell cycle

have demonstrated high expression of the JAK2/STAT3/c-Myc pathway in T-ALL cell lines and samples (20,21). Given that STAT3 mutations have been identified in T-cell malignancies (22), it is worthwhile to investigate whether BP-1-102 could be used to treat T-ALL. In this study, BP-1-102 was administered to T-ALL cell lines (MOLT4 and CUTLL1), and its effects on cell proliferation, colony formation, apoptosis, cell cycle distribution as well as the JAK2/STAT3/c-Myc signaling pathway were examined. The findings revealed that BP-1-102 can inhibit the JAK2/STAT3/c-Myc signaling pathway in T-ALL cells, exerting various antitumor effects. Therefore, BP-1-102 represents a promising targeted antitumor inhibitor.

Materials and methods

Cell culture. MOLT-4 is a cell line of adult T-cell acute lymphoblastic leukemia. CUTLL1 is a cell line of childhood T-cell lymphoblastic lymphoma. Cells were cultured in Roswell Park Memorial Institute (RPMI) 1640 medium containing 10% fetal bovine serum (FBS). All cells were incubated in an incubator (Thermo Scientific, Waltham, MA, USA) containing 95% air and 5% CO_2 at 37˚C.

Reagents and Antibodies. The STAT3-specific inhibitor BP-1-102 was purchased from MedChemExpress (MCE). The chemical structure is shown in Fig. 1A. Antibodies against JAK2 (#3230), STAT3 (#4904), p-STAT3 (Tyr705) (#9145), c-Myc (#5605), Bcl-2 (#2870), Bcl-xL (#2764), Cyclin D1 (#55506) and β-actin (#3700) were purchased from Cell Signaling Technology (CST).

Cell viability assay. The experimental groups were treated with the indicated concentrations of BP-1-102, and the control group was treated with an equal volume of dimethylsulfoxide (DMSO) vehicle for 48 h. Cells were seeded at 105 μl per well in 96-well plates in quadruplicate at a density of $1x10^5$/ml. Ten microliters of Cell Counting Kit-8 (CCK-8) reagent (NCM Biotech, C6005) was added, and the cells were incubated for 3 h at 37˚C. The optical density at 450 nm (OD450) was measured using a spectrophotometer (Thermo Electron, Waltham, MA, USA). Relative cell viability and half-maximal inhibitory concentration (IC_{50}) were calculated.

Cell colony formation assay. Cells were mixed at a density of 4,000/ml in semisolid culture with 30% serum and indicated concentrations of the drug. The semisolid culture system was seeded at 1 mL per dish in 35-mm dishes in triplicate. Petri dishes were incubated for 12 days in a humidified incubator at 37 ˚C. Colonies with more than 50 cells were counted under a microscope (ZEISS, Axio Vert. A1) and photographed.

Cell apoptosis assay. Cells were seeded in 6-well plates in triplicate at a density of $4x10^5$/ml and treated with 0, 15, or 20 μM BP-1-102 for 24 h, ensuring the same concentration of DMSO in every group. Cells were subsequently stained with Annexin V and propidium iodide (PI) dye following the instructions of the Annexin-V-FITC kit (4A Biotech Co., Ltd., Beijing, China). The apoptosis signal was detected by flow cytometry (Cytek, NL-CLC) and processed with FlowJo 10.5.3 software.

Inverted light microscopy. Cells were seeded in 6-well plates at a density of $4x10^5$/ml and treated with 15 μM BP-1-102 or an equal volume of DMSO vehicle. After incubation for 6 h, the cells were observed and photographed using an inverted light microscope (ZEISS, Axio Vert. A1) to search for subcellular structures, such as apoptotic bodies.

Transmission electron microscopy. Cells were seeded in 6-well plates at a density of $4x10^5$/ml and treated with 15 μM BP-1-102 or an equal volume of DMSO vehicle for 6 h. Cells were then fixed in precooled 2.5% glutaraldehyde solution for 24 h. After dehydration, permeation, embedding, sectioning and staining, the samples were prepared. The samples were observed and photographed by a transmission electron microscope (Hitachi TEM system, HT7800).

Cell cycle assay. Cells were seeded in 6-well plates in triplicate at a density of $4x10^5$/ml and treated with 10 μM BP-1-102 or an equal volume of DMSO vehicle for 24 h. Cells were collected and stained with PI dye (4A Biotech Co., Ltd., Beijing, China) after being fixed with ethanol solution. The PI signal was detected by flow cytometry (Cytek, NL-CLC), and cell cycle distribution was processed with ModFit LT 3.1 software.

Western blotting. Cells were seeded in 6-well plates at a density of $1x10^6$/ml and treated with 15 or 20 μM BP-1-102 or an equal volume of DMSO vehicle for 6 h. Total protein was extracted by Radio Immunoprecipitation Assay (RIPA) lysis buffer (with protease inhibitor, phosphatase inhibitor and phenylmethanesulfonyl fluoride added) using a sonicator (Sonics, Newtown, CT, USA). The protein concentration was determined using the Bicinchoninic Acid (BCA) assay (KeyGEN Biotech, KGP902).

Twenty-five micrograms of the cell lysate was subjected to sodium dodecyl sulfate-polyacrylamide gel electrophoresis (SDS-PAGE) and then transferred to polyvinylidene fluoride (PVDF) membranes (Millipore, Boston, MA, USA). The membranes were sequentially incubated with 5% skim milk, primary antibodies and horseradish peroxidase (HRP)-conjugated secondary antibodies (Proteintech, Chicago, IL, USA). Proteins were visualized using an HRP-based chemiluminescence kit (Monad, PW30601S) and Gel Imaging System (Bio-Rad, Alfred Nobel Drive, Hercules, CA, USA). All experiments were repeated thrice. These bands were quantified by densitometry with Scion Image software (ImageJ v1.53s).

Statistical methods. GraphPad Prism 8.0 (GraphPad Software, San Diego, CA, USA) was applied for statistical analysis. Unpaired Student t-test was used to compare normally distributed data from two groups. Dunnett's test was used for multiple comparisons of each drug-treated group versus the control group. Nonlinear regression was used to fit the dose-viability curves and calculate their IC_{50} values. Data are expressed as the mean ± standard deviation. $P<0.05$ was considered statistically significant.

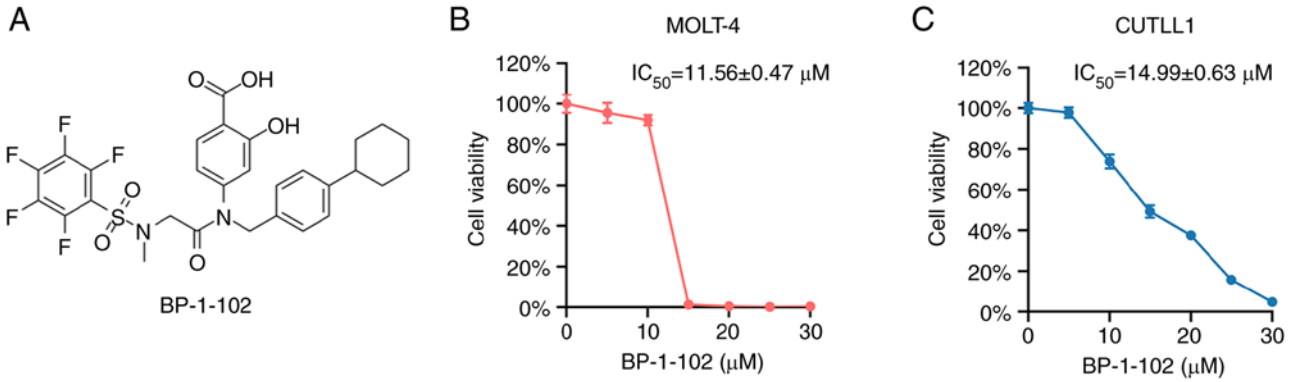

Figure 1. BP-1-102 inhibits cell proliferation. (A) Chemical structure of BP-1-102. (B) Dose-viability curve of BP-1-102 in MOLT-4 cells. IC_{50} is the half-maximal inhibitory concentration. (C) Dose-viability curve of BP-1-102 in CUTLL1 cells.

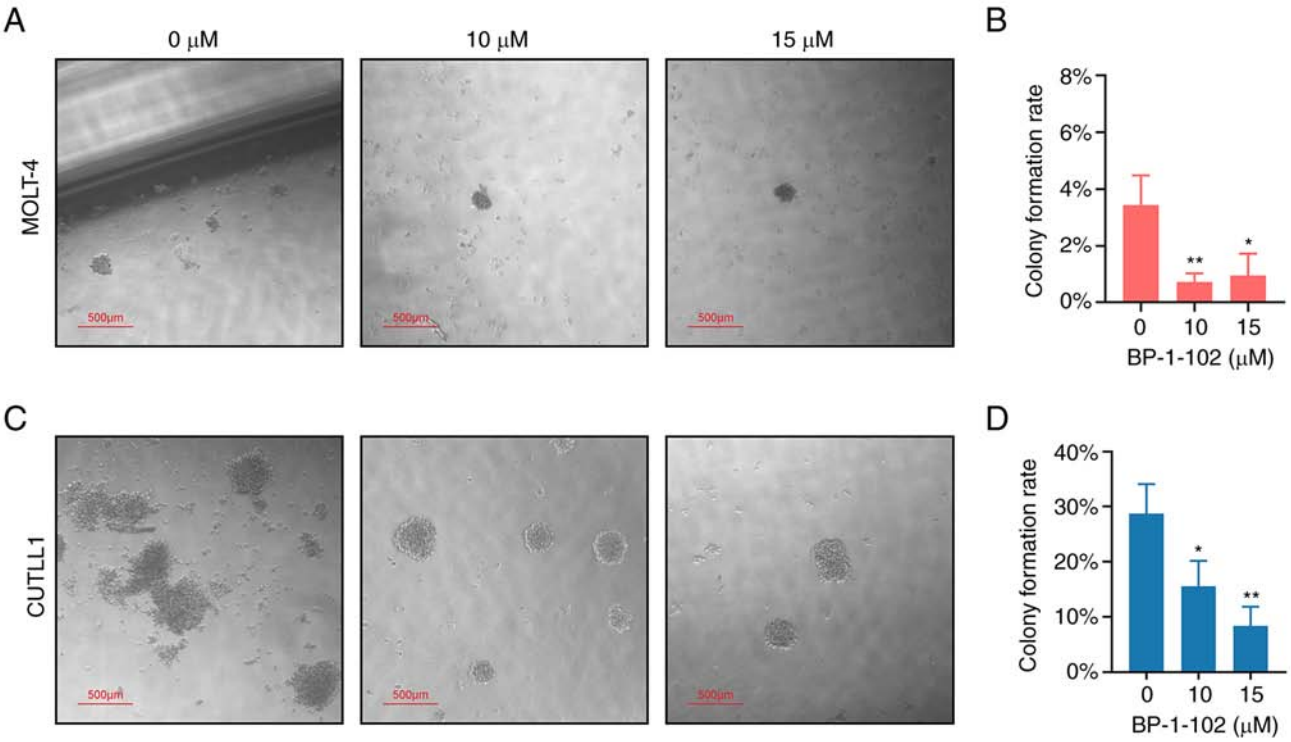

Figure 2. BP-1-102 inhibits cell colony formation. (A) Micrographs of cell colonies of MOLT-4. Clusters >200 μm in diameter are defined as cell colonies. Scale bar, 500 μm. (B) Bar chart of the cell colony formation rate of MOLT-4. (C) Micrographs of cell colonies of CUTLL1. Scale bar, 500 μm. (D) Bar chart of the cell colony formation rate of CUTLL1. *P<0.05 and **P<0.01 compared with the 0 μM group.

Results

BP-1-102 inhibited cell proliferation. To test the antitumor effect of BP-1-102, we first performed a CCK-8 assay to examine the effect of BP-1-102 on T-ALL cell proliferation. We treated the T-ALL cell line with a gradient concentration of the drug for 48 h before the CCK-8 assay was performed. The results showed that BP-1-102 inhibited cell proliferation, and the inhibitory effect was enhanced as the drug concentration increased (Fig. 1B and C). The half-maximal inhibitory concentration (IC_{50}) of BP-1-102 in the MOLT-4 cell line was 11.56±0.47 μM (Fig. 1B). The half-maximal inhibitory concentration (IC_{50}) of BP-1-102 in the CUTLL1 cell line was 14.99±0.63 μM (Fig. 1C). The cell viability of MOLT-4 was slightly lower than that of CUTLL1 due to cell line based differences.

BP-1-102 inhibited cell colony formation. In addition to cell proliferation, we also examined the effect of BP-1-102 on the colony formation ability of T-ALL cell lines. We cultured T-ALL cells with methylcellulose semisolid medium containing the indicated drug concentration for 12 days and counted the number of colonies. The results showed that BP-1-102 inhibited the colony formation ability of T-ALL cells (Fig. 2). The colony formation rate of MOLT-4 was much lower than that of CUTLL1, and the size of its colonies was much smaller (Fig. 2). A significant decrease in the colony formation rate of the 10 and 15 μM groups of MOLT-4 was observed by counting the number of colonies under a microscope (Fig. 2B). The colony formation capacity of CUTLL1 was higher with dense colonies noted in the control group (Fig. 2C). A gradient decrease

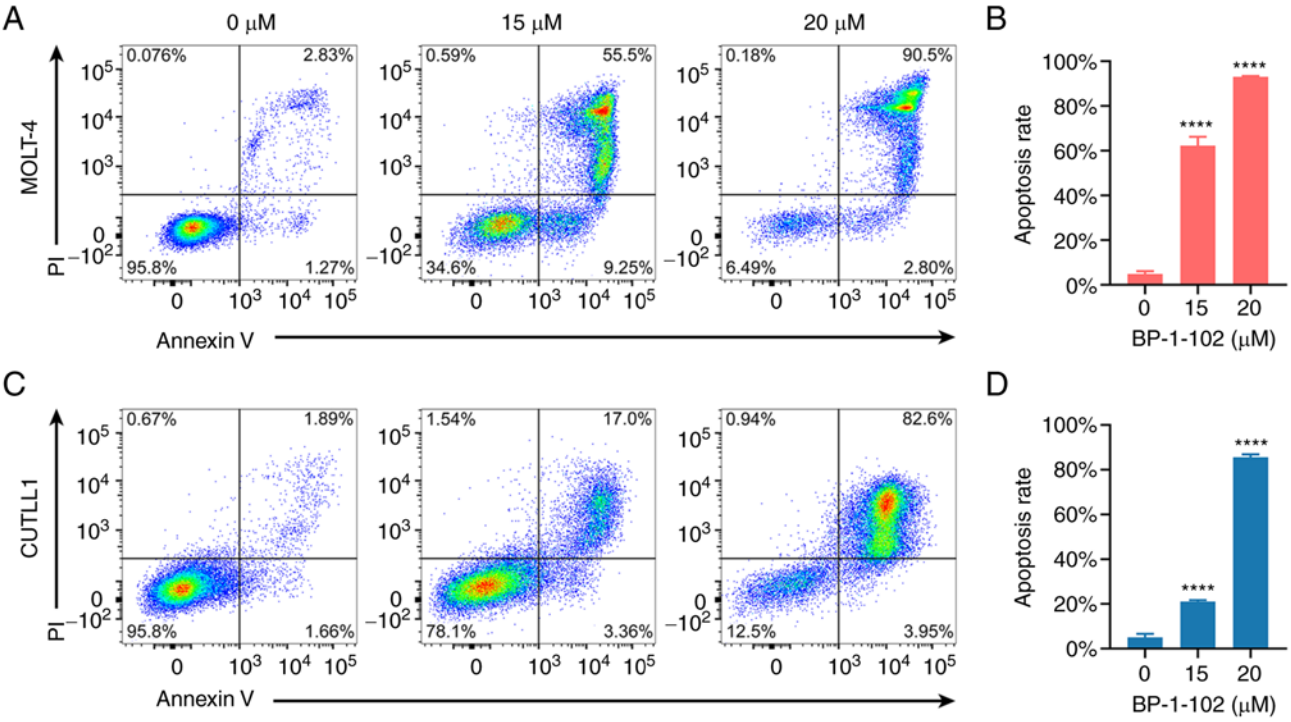

Figure 3. BP-1-102 induces apoptosis. (A) Flow cytometry scatter plots of MOLT-4. The horizontal axis is the Annexin V fluorescence channel, and the vertical axis is the PI fluorescence channel. Living cells are in the lower left quadrant; early apoptotic cells are in the lower right quadrant; late apoptotic cells and necrotic cells are in the upper right quadrant. (B) Bar chart of apoptosis rates of MOLT-4. (C) Flow cytometry scatter plots of CUTLL1. (D) Bar chart of apoptosis rates of CUTLL1. ****P<0.0001 compared with the 0 μM group.

in colony formation rate of CUTLL1 was observed in the 10 and 15 μM groups (Fig. 2D).

BP-1-102 induced cell apoptosis. To explore the mechanism of the antitumor effect of BP-1-102, we examined the apoptosis-inducing effect of BP-1-102 in T-ALL cell lines by flow cytometry. After incubating the T-ALL cell line with BP-1-102 for 24 h, the cells were labeled with Annexin V and PI dye, and the fluorescence intensity of each cell was measured by flow cytometry. The results showed that BP-1-102 induced apoptosis in T-ALL cells and the apoptosis-inducing effect was enhanced with increasing drug concentration (Fig. 3). Significant MOLT-4 and CUTLL1 cell apoptosis were noted in both the 15 and 20 μM groups; in particular, the 20 μM group showed very high apoptosis rates of 93.00±0.32% and 85.66±1.00% in the two cell lines, respectively (Fig. 3B, D). The vast majority of apoptosis in MOLT-4 and CUTLL1 cells exhibited late apoptosis (Fig. 3A and C). Considering that 20 μM BP-1-102 could lead to such a high apoptosis rate, we concluded that among the various cytotoxic and antitumor effects of BP-1-102, the induction of apoptosis represented its most dominant role.

To demonstrate that apoptosis occurred in T-ALL cells after BP-1-102 treatment, we incubated the cells with 15 μM BP-1-102 for 6 h and then observed cell morphology using inverted light microscopy and transmission electron microscopy (Fig. 4). Healthy cells in the control group were round and full under a light microscope, and healthy organelles, such as mitochondria, were visible under a transmission electron microscope. In contrast, cells in the drug-treated group showed subcellular structural features of apoptosis and necrosis: apoptotic bodies, cell shrinkage, swollen mitochondria, crescent-shaped chromatin, petal-like chromatin, pyknosis (condensed nuclei) and karyorrhexis (fragmented nuclei). Morphological results showed that apoptosis occurred in the drug-treated cells (Fig. 4).

BP-1-102 caused cell cycle arrest at the G_0/G_1 phase. To explore the mechanism of the antitumor effect of BP-1-102, we examined the effect of BP-1-102 on the cell cycle distribution of T-ALL cell lines by flow cytometry. MOLT-4 and CUTLL1 cells were treated with 10 μM BP-1-102 or an equal volume of DMSO for 24 h, fixed in ethanol and then stained with PI dye. The PI fluorescence intensity of each cell was measured by flow cytometry. The results showed that BP-1-102 blocked the cell cycle at the G_0/G_1 phase (Fig. 5). The proportion of G_0/G_1 phase cells in MOLT-4 increased from 33.67±0.74% to 57.27±1.06%, and the proportion of S phase cells decreased from 65.59±1.11% to 41.16±0.92% (Fig. 5A and B). The percentage of G_0/G_1 phase cells in CUTLL1 increased from 26.24%±0.84% to 38.60±1.40%, and the percentage of S phase cells decreased from 73.64±0.76% to 59.07±2.64% (Fig. 5C and D). The altered cell cycle distribution increased the proportion of resting cells, decreased the proportion of proliferating cells and slowed the proliferation of the cell population as a whole. In addition, the results showed that there was no sub-G1 peak in the drug-treated group, but a higher percentage of cellular debris.

BP-1-102 suppressed the JAK2/STAT3/c-Myc signaling pathway. To investigate the mechanisms by which BP-1-102 exerted the various effects described above, the expression

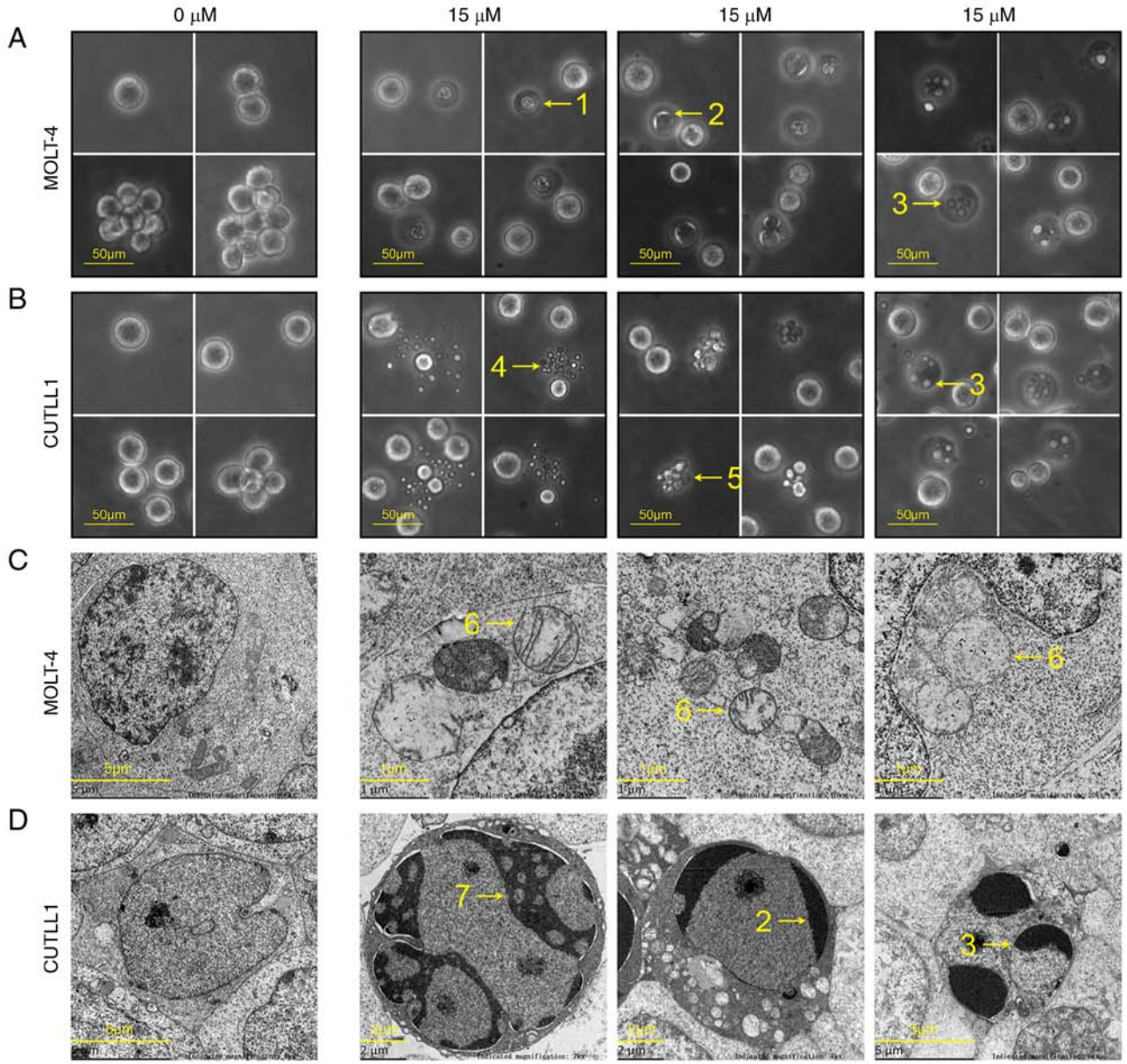

Figure 4. BP-1-102 induces apoptosis. Morphological assessments were performed using an inverted light microscope in (A) MOLT-4 and (B) CUTLL1 cells (scale bar, 50 μm). Morphological assessments were performed by transmission electron microscopy in (C) MOLT-4 (scale bars from left to right, 5, 1, 1 and 1 μm, respectively) (D) CUTLL1 cells (scale bars from left to right, 5, 2, 2 and 5 μm, respectively). The annotations are as follows: 1=pyknosis (condensed nuclei); 2=crescent-shaped chromatin; 3=karyorrhexis (fragmented nuclei); 4=apoptotic bodies; 5=cell shrinkage; 6=swollen mitochondria; and 7=petal-like chromatin.

levels of the factors involved in the JAK2-STAT3 pathway and several downstream proteins were measured by Western blotting. The results showed that BP-1-102 downregulated the JAK2-STAT3 pathway and significantly inhibited c-Myc protein expression (Fig. 6).

Although the inhibitory effects of BP-1-102 on cell proliferation were slightly different between MOLT-4 and CUTLL1 cells, the basal expression levels of the JAK2/STAT3/c-Myc pathway were high in both cell lines. For both MOLT-4 and CUTLL1 cells, BP-1-102 significantly inhibited JAK2 expression in a dose-dependent manner. This finding reflected the interaction between STAT3 and JAK2 (Fig. 6A and B). The effect of BP-1-102 on total STAT3 was not apparent and only differed significantly in the drug-treated MOLT-4 group (Fig. 6C and D). Regretfully, phosphorylated STAT3 was likely minimally expressed in both T-ALL cell lines and was not detected by Western blotting in either (data not shown). Perhaps changes in phosphorylated STAT3 levels can be detected by flow cytometry or enzyme-linked immunosorbent assay (ELISA) kits.

As a classical oncogene that promotes tumor cell proliferation, c-Myc is a downstream gene of STAT3. Both the bands of c-Myc and the histogram of its quantification reflected a significant reduction in c-Myc expression in the drug-treated groups, exhibiting a typical stepwise decrease. The expression of c-Myc in the 20 μM groups was only approximately 10% of that in the control group (Fig. 6E and F). The antitumor effects of BP-1-102 on T-ALL cell lines were likely to result from direct inhibition of STAT3 phosphorylation and the subsequent indirect inhibition of c-Myc protein.

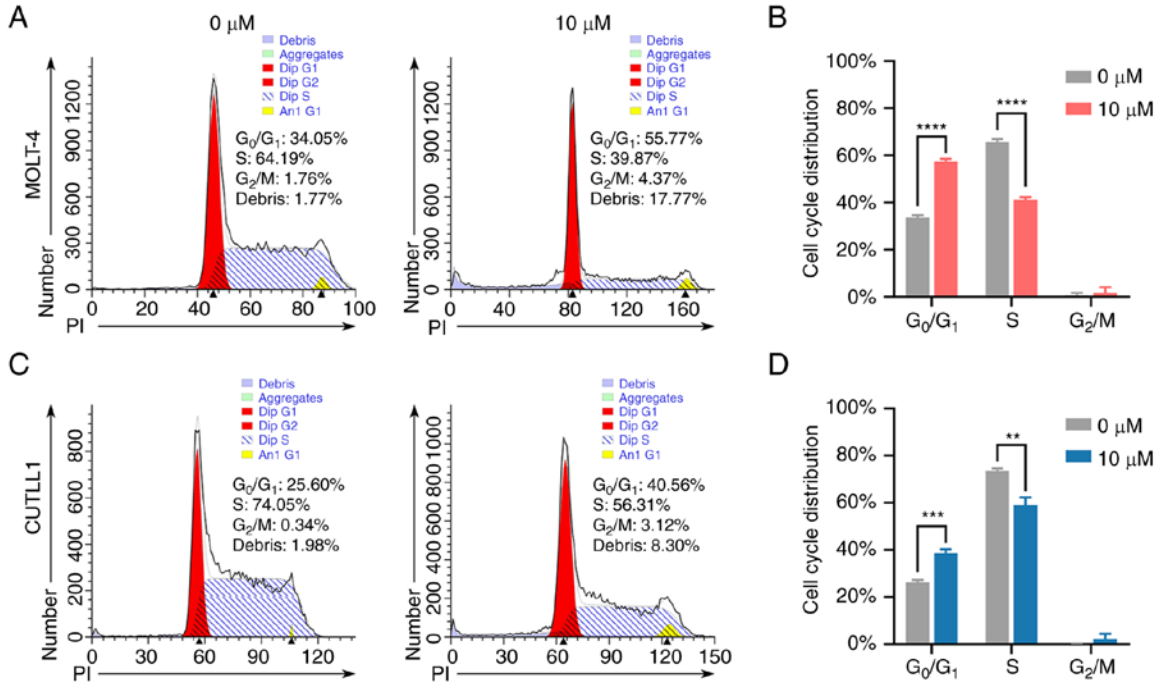

Figure 5. BP-1-102 causes cell cycle arrest at the G_0/G_1 phase. (A) Flow cytometry histogram of PI fluorescence intensity of MOLT-4. (B) Bar chart of the cell cycle distribution of MOLT-4. (C) Flow cytometry histogram of PI fluorescence intensity of CUTLL1. (D) Bar chart of the cell cycle distribution of CUTLL1. **P<0.01, ***P<0.001 and ****P<0.0001.

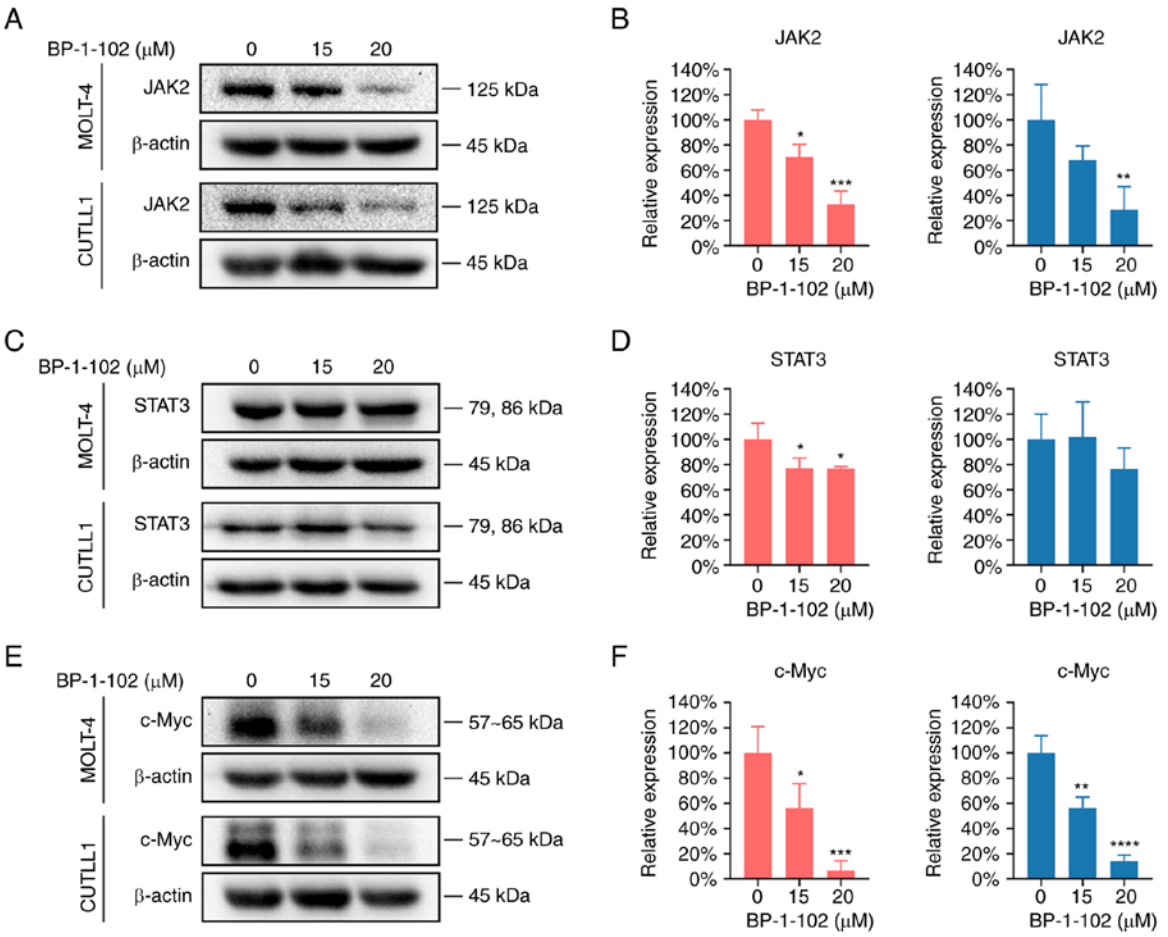

Figure 6. BP-1-102 suppresses the JAK2/STAT3/c-Myc signaling pathway. (A) Western blotting band of JAK2. (B) Bar chart of relative JAK2 expression in MOLT-4 (left) and CUTLL1 (right) cells. (C) Western blotting band of STAT3. (D) Bar chart of relative STAT3 expression in MOLT-4 (left) and CUTLL1 (right) cells. (E) Western blotting band of c-Myc. (F) Bar chart of relative c-Myc expression in MOLT-4 (left) and CUTLL1 (right) cells. *P<0.05, **P<0.01, ***P<0.001 and ****P<0.0001 compared with the 0 μM group.

Discussion

T-cell acute lymphoblastic leukemia is a highly aggressive and heterogeneous hematological malignancy. Over the past decades, a variety of targeted drugs have been developed to target the pathological process of T-ALL. Unfortunately, none of the new targeted drugs have been approved as first-line treatment options. The research and development of new targeted drugs for T-ALL are translationally important.

The JAK-STAT signaling pathway plays an important role in leukemia pathogenesis and could be used as a potential target for drug therapy. Activation of STAT proteins, particularly STAT5 and STAT3, plays a crucial role in the pathogenesis of lymphoid and myeloid malignancies (23). Human T-cell lymphotropic virus type I (HTLV-I) is a cause of adult T-cell leukemia. The JAK-STAT signaling pathway is constitutively activated in HTLV-I-mediated malignant T cells (24). STAT3 is constitutively activated in lymphoblastoid-like cells and Burkitt's lymphoma cells that are EBV-positive or permanently expressing interleukin-10 (25). Recurrent STAT3 mutations were identified in 40% of T-cell large granular lymphocytic leukemia cases. These mutations increase the transcriptional activity of STAT3 and lead to the upregulation of STAT3 target genes, such as Bcl-2-like protein 1 (BCL2L1) and JAK2 (26,27). STAT3 mutations were found in 4 of 258 patients with T-cell tumors, and the mutations were confined to malignant cells. These mutations in STAT3 (Y640F) lead to constitutive activation of STAT3 and malignant hematopoiesis *in vivo* (28). As demonstrated by Western blotting, Cheng *et al*. found significantly increased JAK2 and STAT3 expression in T-ALL patient samples compared with healthy controls (20). Taken together, STAT3 emerges as a potential therapeutic target for T-ALL.

BP-1-102 is a homologue of S3I-201.1066 (29) obtained by computer-aided optimization. As a ligand for the SH2 domain of STAT3, BP-1-102 can compete with the pTyr of the upstream molecule, subsequently interfering with the binding of pTyr to the SH2 domain of STAT3 and, as a result, blocking STAT3 phosphorylation and dimerization (17). We administered gradient concentrations of BP-1-102 to T-ALL cell lines and examined its antitumor properties. The results showed that BP-1-102 inhibited tumor cell proliferation and cell colony formation, induced apoptosis and blocked the cell cycle at the G_0/G_1 phase. The antiproliferative and apoptosis-inducing effects were dose-dependent. In summary, BP-1-102 represents a promising targeted antitumor medication that is expected to be used in clinical trials.

When the apoptosis rates were detected by flow cytometry, the cells had been treated for 24 h, when late apoptosis dominated in MOLT-4 and CUTLL1 (Fig. 3). Yet we later found that incubation for 6 h was most suitable for morphological analysis, when the cells exhibited the most typical apoptotic morphological features such as apoptotic bodies (Fig. 4B). Both Bcl-2 and Bcl-xL are classical anti-apoptotic oncogenes downstream of STAT3 (30). The expression levels of Bcl-2 and Bcl-xL were slightly reduced by BP-1-102 treatment, which contributed to apoptosis. Yet such inhibition effects were weak and poorly reproducible (data not shown).

Cyclin D1 drives cell cycle progression from G0/G1 phase to S phase. Overexpressed Cyclin D1 has oncogenic effects (31). Xiaoxia Jiang *et al* once administered BP-1-102 to gastric cancer cell line AGS cells and found that Cyclin D1 was downregulated, although the cell cycle distribution of AGS cells was not affected significantly (18). We hypothesized that BP-1-102 exerted its cell cycle-blocking effects on T-ALL cells by inhibition of cyclin D1 downstream of STAT3 (Fig. 5). Regrettably, cyclin D1 expression levels examined by Western blotting were not significantly reduced (data not shown).

c-Myc is a transcription factor that is highly expressed in over 70% of cancers. As a very important oncogene with a broad role, c-Myc is involved in the regulation of proliferation, differentiation, apoptosis and the cell cycle in many tumors (32). c-Myc also promotes tumor angiogenesis, metastasis and chemoresistance (33). c-Myc is a downstream gene regulated by STAT3. The STAT3/c-Myc axis is involved in the oncogenesis, progression, metabolism and therapeutic response of a variety of cancers (34-37). Haizhi Yu *et al*. found that c-Myc expression levels were increased in patients' T-ALL cells as well as Jurkat and DU528 T-ALL cell lines compared with peripheral blood mononuclear cells (PBMCs) from healthy donors (21).

In the present study, c-Myc protein expression was completely inhibited in the high-concentration group (Fig. 6). The antiproliferative, apoptosis-inducing and cell cycle blocking effects of BP-1-102 in T-ALL were mainly mediated through indirect inhibition of c-Myc (Fig. 6). The principal mechanism by which BP-1-102 exerts its antitumor effects in T-ALL cell lines is the suppression of the JAK2/STAT3/c-Myc oncogenic pathway (Fig. 6). Considering the driver role of c-Myc in many types of cancers, BP-1-102 may be applied to a wide range of other tumors.

The shortcoming of this study should be noted. Specifically, samples from T-ALL patients have not been studied, and *in vivo* studies have not been conducted. Such experiments may further validate the antitumor effects and safety of BP-1-102.

BP-1-102 exerts anti-inflammatory effects in addition to its antitumor effects. Qi-Ying Wu *et al* demonstrated that BP-1-102 inhibited JAK2/STAT3/NF-κB pathway activation in a mouse abdominal aortic aneurysm model, thereby reducing the expression of proinflammatory cytokines, decreasing inflammatory cell infiltration, and ultimately impeding the development and progression of abdominal aortic aneurysms (38). Zhixian Jiang *et al*. demonstrated that BP-1-102 suppressed the JAK/STAT3/NF-κB pathway in intracranial aneurysms, reduced the vascular inflammatory response, alleviated the symptoms of intracranial aneurysms and prevented their rupture (39,40).

Chronic inflammation is associated with the oncogenesis of many tumors, the most typical of which is hepatocellular carcinoma. Transcription factors NF-κB and STAT3 are both implicated in the development of hepatocellular carcinoma (41,42). Regarding the mechanism of inflammation-induced malignant transformation in cancers, such as hepatocellular carcinoma, BP-1-102 may provide researchers with new clues. Necroptosis is a type of pro-inflammatory cell death (43). Induction of necroptosis may bypass treatment resistance in cancers and accelerate the development of novel therapeutic strategies for apoptosis-resistant leukemia (44). Whether BP-1-102 plays a role in inducing necroptosis in leukemia is worth investigating in the future.

In summary, we demonstrated that the JAK2/STAT3/c-Myc pathway is necessary for the survival and maintenance of T-ALL cells. In T-ALL cell lines, BP-1-102 suppressed the JAK2/STAT3/c-Myc signaling pathway, thus inhibiting

cell proliferation and colony formation, inducing apoptosis and blocking the cell cycle at the G_0/G_1 phase. BP-1-102 is a promising targeted inhibitor that offers an effective option for targeted therapy in T-ALL. BP-1-102 and its potential derivatives deserve to be explored in *in vivo* experiments and clinical trials.

Acknowledgements

We wish to thank Professor Guangsen Zhang (Department of Hematology, The Second Xiangya Hospital, Central South University, Changsha, China) for his patient guidance and great support. We wish to thank Dr Weiwei Yang (School of Basic Medical Sciences, Harbin Medical University, Harbin, China) for her kind help with TEM figure labeling.

Funding

This work was supported by the National Natural Science Foundation of China (grant no. 82070175).

Availability of data and materials

All data generated or analyzed during this study are included in this published article.

Authors' contributions

CY and ZC conceptualized this study. CY conducted the experiments. CY, XR, YZ, HZ, CW, ZC and HP were involved in the data analysis and validation. CY and ZC confirmed the authenticity of all the raw data. CY and ZC wrote the manuscript. HP provided project administration and funding. All authors have read and approved the final manuscript.

Ethics approval and consent to participate

Not applicable.

Patient consent for publication

Not applicable.

Competing interests

The authors declare that they have no competing interests.

References

1. Belver L and Ferrando A: The genetics and mechanisms of T cell acute lymphoblastic leukaemia. Nat Rev Cancer 16: 494-507, 2016.
2. Girardi T, Vicente C, Cools J and De Keersmaecker K: The genetics and molecular biology of T-ALL. Blood 129: 1113-1123, 2017.
3. Hunger SP and Mullighan CG: Acute lymphoblastic leukemia in children. N Engl J Med 373: 1541-1552, 2015.
4. Hunger SP, Lu X, Devidas M, Camitta BM, Gaynon PS, Winick NJ, Reaman GH and Carroll WL: Improved survival for children and adolescents with acute lymphoblastic leukemia between 1990 and 2005: A report from the children's oncology group. J Clin Oncol 30: 1663-1669, 2012.
5. Bhojwani D and Pui CH: Relapsed childhood acute lymphoblastic leukaemia. Lancet Oncol 14: e205-e217, 2013.
6. Reismüller B, Attarbaschi A, Peters C, Dworzak MN, Pötschger U, Urban C, Fink FM, Meister B, Schmitt K, Dieckmann K, *et al*: Long-term outcome of initially homogenously treated and relapsed childhood acute lymphoblastic leukaemia in Austria--a population-based report of the Austrian Berlin-Frankfurt-Münster (BFM) study group. Br J Haematol 144: 559-570, 2009.
7. Pocock R, Farah N, Richardson SE and Mansour MR: Current and emerging therapeutic approaches for T-cell acute lymphoblastic leukaemia. Br J Haematol 194: 28-43, 2021.
8. Hu X, Li J, Fu M, Zhao X and Wang W: The JAK/STAT signaling pathway: From bench to clinic. Signal Transduct Target Ther 6: 402, 2021.
9. Aittomäki S and Pesu M: Therapeutic targeting of the Jak/STAT pathway. Basic Clin Pharmacol Toxicol 114: 18-23, 2014.
10. O'Shea JJ, Schwartz DM, Villarino AV, Gadina M, McInnes IB and Laurence A: The JAK-STAT pathway: Impact on human disease and therapeutic intervention. Annu Rev Med 66: 311-328, 2015.
11. Ashizawa T, Akiyama Y, Miyata H, Iizuka A, Komiyama M, Kume A, Omiya M, Sugino T, Asai A, Hayashi N, *et al*: Effect of the STAT3 inhibitor STX-0119 on the proliferation of a temozolomide-resistant glioblastoma cell line. Int J Oncol 45: 411-418, 2014.
12. Song H, Wang R, Wang S and Lin J: A low-molecular-weight compound discovered through virtual database screening inhibits Stat3 function in breast cancer cells. Proc Natl Acad Sci USA 102: 4700-4705, 2005.
13. Fuh B, Sobo M, Cen L, Josiah D, Hutzen B, Cisek K, Bhasin D, Regan N, Lin L, Chan C, *et al*: LLL-3 inhibits STAT3 activity, suppresses glioblastoma cell growth and prolongs survival in a mouse glioblastoma model. Br J Cancer 100: 106-112, 2009.
14. Nie Y, Li Y and Hu S: A novel small inhibitor, LLL12, targets STAT3 in non-small cell lung cancer in vitro and in vivo. Oncol Lett 16: 5349-5354, 2018.
15. Liu A, Liu Y, Jin Z, Hu Q, Lin L, Jou D, Yang J, Xu Z, Wang H, Li C and Lin J: XZH-5 inhibits STAT3 phosphorylation and enhances the cytotoxicity of chemotherapeutic drugs in human breast and pancreatic cancer cells. PLoS One 7: e46624, 2012.
16. Kim MJ, Nam HJ, Kim HP, Han SW, Im SA, Kim TY, Oh DY and Bang YJ: OPB-31121, a novel small molecular inhibitor, disrupts the JAK2/STAT3 pathway and exhibits an antitumor activity in gastric cancer cells. Cancer Lett 335: 145-152, 2013.
17. Zhang X, Yue P, Page BD, Li T, Zhao W, Namanja AT, Paladino D, Zhao J, Chen Y, Gunning PT and Turkson J: Orally bioavailable small-molecule inhibitor of transcription factor Stat3 regresses human breast and lung cancer xenografts. Proc Natl Acad Sci USA 109: 9623-9628, 2012.
18. Jiang X, Tang J, Wu M, Chen S, Xu Z, Wang H, Wang H, Yu X, Li Z and Teng L: BP-1-102 exerts an antitumor effect on the AGS human gastric cancer cell line through modulating the STAT3 and MAPK signaling pathways. Mol Med Rep 19: 2698-2706, 2019.
19. Belton A, Xian L, Huso T, Koo M, Luo LZ, Turkson J, Page BD, Gunning PT, Liu G, Huso DL and Resar LM: STAT3 inhibitor has potent antitumor activity in B-lineage acute lymphoblastic leukemia cells overexpressing the high mobility group A1 (HMGA1)-STAT3 pathway. Leuk Lymphoma 57: 2681-2684, 2016.
20. Cheng Z, Yi Y, Xie S, Yu H, Peng H and Zhang G: The effect of the JAK2 inhibitor TG101209 against T cell acute lymphoblastic leukemia (T-ALL) is mediated by inhibition of JAK-STAT signaling and activation of the crosstalk between apoptosis and autophagy signaling. Oncotarget 8: 106753-106763, 2017.
21. Yu H, Yin Y, Yi Y, Cheng Z, Kuang W, Li R, Zhong H, Cui Y, Yuan L, Gong F, *et al*: Targeting lactate dehydrogenase A (LDHA) exerts antileukemic effects on T-cell acute lymphoblastic leukemia. Cancer Commun (Lond) 40: 501-517, 2020.
22. Pencik J, Pham HT, Schmoellerl J, Javaheri T, Schlederer M, Culig Z, Merkel O, Moriggl R, Grebien F and Kenner L: JAK-STAT signaling in cancer: From cytokines to non-coding genome. Cytokine 87: 26-36, 2016.
23. Vainchenker W and Constantinescu SN: JAK/STAT signaling in hematological malignancies. Oncogene 32: 2601-2613, 2013.
24. Migone TS, Lin JX, Cereseto A, Mulloy JC, O'Shea JJ, Franchini G and Leonard WJ: Constitutively activated Jak-STAT pathway in T cells transformed with HTLV-I. Science 269: 79-81, 1995.
25. Weber-Nordt RM, Egen C, Wehinger J, Ludwig W, Gouilleux-Gruart V, Mertelsmann R and Finke J: Constitutive activation of STAT proteins in primary lymphoid and myeloid leukemia cells and in Epstein-Barr virus (EBV)-related lymphoma cell lines. Blood 88: 809-816, 1996.

26. Ohgami RS, Ma L, Merker JD, Martinez B, Zehnder JL and Arber DA: STAT3 mutations are frequent in CD30+ T-cell lymphomas and T-cell large granular lymphocytic leukemia. Leukemia 27: 2244-2247, 2013.
27. Koskela HL, Eldfors S, Ellonen P, van Adrichem AJ, Kuusanmäki H, Andersson EI, Lagström S, Clemente MJ, Olson T, Jalkanen SE, *et al*: Somatic STAT3 mutations in large granular lymphocytic leukemia. N Engl J Med 366: 1905-1913, 2012.
28. Couronné L, Scourzic L, Pilati C, Della Valle V, Duffourd Y, Solary E, Vainchenker W, Merlio JP, Beylot-Barry M, Damm F, *et al*: STAT3 mutations identified in human hematologic neoplasms induce myeloid malignancies in a mouse bone marrow transplantation model. Haematologica 98: 1748-1752, 2013.
29. Zhang X, Yue P, Fletcher S, Zhao W, Gunning PT and Turkson J: A novel small-molecule disrupts Stat3 SH2 domain-phosphotyrosine interactions and Stat3-dependent tumor processes. Biochem Pharmacol 79: 1398-1409, 2010.
30. Pistritto G, Trisciuoglio D, Ceci C, Garufi A and D'Orazi G: Apoptosis as anticancer mechanism: Function and dysfunction of its modulators and targeted therapeutic strategies. Aging 8: 603-619, 2016.
31. Montalto FI and De Amicis F: Cyclin D1 in cancer: A molecular connection for cell cycle control, adhesion and invasion in tumor and stroma. Cells 9: 2648, 2020.
32. Madden SK, de Araujo AD, Gerhardt M, Fairlie DP and Mason JM: Taking the Myc out of cancer: Toward therapeutic strategies to directly inhibit c-Myc. Mol Cancer 20: 3, 2021.
33. Ala M: Target c-Myc to treat pancreatic cancer. Cancer Biol Ther 23: 34-50, 2022.
34. Mo M, Tong S, Yin H, Jin Z, Zu X and Hu X: SHCBP1 regulates STAT3/c-Myc signaling activation to promote tumor progression in penile cancer. Am J Cancer Res 10: 3138-3156, 2020.
35. Gao S, Chen M, Wei W, Zhang X, Zhang M, Yao Y, Lv Y, Ling T, Wang L and Zou X: Crosstalk of mTOR/PKM2 and STAT3/c-Myc signaling pathways regulate the energy metabolism and acidic microenvironment of gastric cancer. J Cell Biochem 120: 1193-1202, 2018.
36. Ning R, Chen G, Fang R, Zhang Y, Zhao W and Qian F: Diosmetin inhibits cell proliferation and promotes apoptosis through STAT3/c-Myc signaling pathway in human osteosarcoma cells. Biol Res 54: 40, 2021.
37. Zhu Y and Feng Y: GRAIL inhibits the growth, migration and invasion of lung adenocarcinoma cells by modulating STAT3/C-MYC signaling pathways. J BUON 26: 353-358, 2021.
38. Wu QY, Cheng Z, Zhou YZ, Zhao Y, Li JM, Zhou XM, Peng HL, Zhang GS, Liao XB and Fu XM: A novel STAT3 inhibitor attenuates angiotensin II-induced abdominal aortic aneurysm progression in mice through modulating vascular inflammation and autophagy. Cell Death Dis 11: 131, 2020.
39. Jiang Z, Huang J, You L, Zhang J and Li B: Pharmacological inhibition of STAT3 by BP-1-102 inhibits intracranial aneurysm formation and rupture in mice through modulating inflammatory response. Pharmacol Res Perspect 9: e00704, 2021.
40. Jiang Z, Huang J, You L and Zhang J: Protective effects of BP-1-102 against intracranial aneurysms-induced impairments in mice. J Drug Target 29: 974-982, 2021.
41. Berasain C, Castillo J, Perugorria MJ, Latasa MU, Prieto J and Avila MA: Inflammation and liver cancer: new molecular links. Ann N Y Acad Sci 1155: 206-221, 2009.
42. He G and Karin M: NF-κB and STAT3-key players in liver inflammation and cancer. Cell Res 21: 159-168, 2011.
43. Negroni A, Colantoni E, Cucchiara S and Stronati L: Necroptosis in intestinal inflammation and cancer: New concepts and therapeutic perspectives. Biomolecules 10: 1431, 2020.
44. Huang X, Xiao F, Li Y, Qian W, Ding W and Ye X: Bypassing drug resistance by triggering necroptosis: Recent advances in mechanisms and its therapeutic exploitation in leukemia. J Exp Clin Cancer Res 37: 310, 2018.